

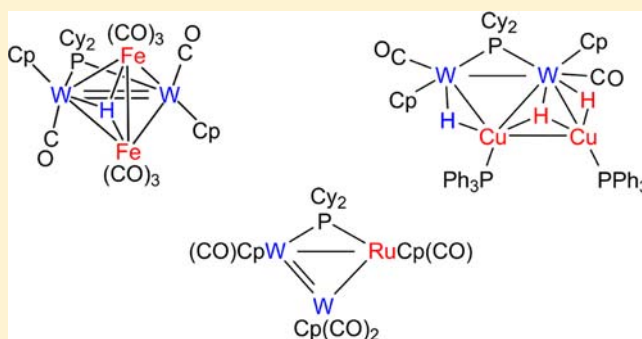
Heterometallic Derivatives of the Unsaturated Ditungsten Hydride $[\text{W}_2(\eta^5\text{-C}_5\text{H}_5)_2(\text{H})(\mu\text{-PCy}_2)(\text{CO})_2]$

M. Angeles Alvarez, M. Esther García, Miguel A. Ruiz,* Adrián Toyos, and M. Fernanda Vega

Departamento de Química Orgánica e Inorgánica/IUQOEM, Universidad de Oviedo, E-33071 Oviedo, Spain

S Supporting Information

ABSTRACT: The title complex reacted with different transition-metal (M) complexes to give heterometallic clusters with W_2M and W_2M_2 metal cores. The reaction with $[\text{Fe}_2(\text{CO})_9]$ in THF at room temperature gave a mixture of the heterodinuclear compound $[\text{FeWCp}(\mu\text{-PCy}_2)(\text{CO})_6]$ and the tetrahedral clusters $[\text{Fe}_2\text{W}_2\text{Cp}_2(\mu_3\text{-H})(\mu\text{-PCy}_2)(\text{CO})_8]$ ($\text{W}\text{--}\text{W} = 2.704(1)$ Å) and $[\text{Fe}_2\text{W}_2\text{Cp}_2(\mu\text{-H})(\mu\text{-PCy}_2)(\mu\text{-CO})(\text{CO})_8]$ ($\text{W}\text{--}\text{W} = 3.058(5)$ Å). In contrast, its reaction with $[\text{Ru}_3(\text{CO})_{12}]$ under ultraviolet–visible (UV–Vis) irradiation gave only the heterodinuclear complex $[\text{RuWCp}(\mu\text{-PCy}_2)(\text{CO})_6]$. The title complex also reacted readily with $[\text{M}(\text{CO})_6]$ ($\text{M} = \text{Cr}, \text{Mo}, \text{W}$) in toluene solution under UV–Vis irradiation, but the main product was the known tetracarbonyl complex $[\text{W}_2\text{Cp}_2(\mu\text{-H})(\mu\text{-PCy}_2)(\text{CO})_4]$, except in the reaction with $[\text{W}(\text{CO})_6]$, the latter also yielding the expected 46-electron cluster $[\text{W}_3\text{Cp}_2(\mu_3\text{-H})(\mu\text{-PCy}_2)(\text{CO})_7]$ in 40% yield. The title complex reacted under visible–UV irradiation with different metal–metal bonded dimers in toluene solution, but only with $[\text{Ru}_2\text{Cp}_2(\text{CO})_4]$ a heterometallic cluster was obtained, with composition $[\text{RuW}_2\text{Cp}_3(\mu\text{-PCy}_2)(\text{CO})_4]$. Its reaction with the tetrahydroborate complex $[\text{Cu}(\text{BH}_4)(\text{PPh}_3)_2]$ led to the insertion of two $\text{CuH}(\text{PPh}_3)$ fragments and release of $\text{BH}_3\cdot\text{PPh}_3$, to give the tetranuclear cluster $[\text{Cu}_2\text{W}_2\text{Cp}_2(\mu\text{-H})_3(\mu\text{-PCy}_2)(\text{CO})_2(\text{PPh}_3)_2]$, which exists in solution as an equilibrium mixture of two isomers.

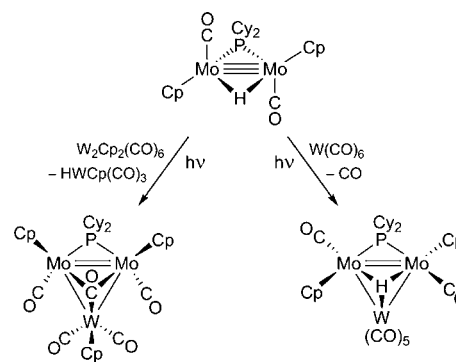


INTRODUCTION

Organometallic compounds having hydride ligands bridging over metal–metal multiple bonds are usually very active species that react under mild conditions with a great variety of molecules to give products that cannot be prepared via other routes. This is well-illustrated by the rich chemistry developed around the complexes $[\text{Os}_3(\mu\text{-H})_2(\text{CO})_{10}]$,¹ $[\text{Re}_2(\mu\text{-H})_2(\text{CO})_8]$,² and $[\text{Mn}_2(\mu\text{-H})_2(\text{CO})_6(\mu\text{-L}_2)]$,³ ($\text{L}_2 = (\text{EtO})_2\text{POP}(\text{OEt})_2$ or $\text{Ph}_2\text{PCH}_2\text{PPh}_2$), all of which display an unsaturated $\text{M}_2(\mu\text{-H})_2$ moiety with a formal bond order of 2, or that around the 30-electron hydrides $[\text{M}_2\text{Cp}^*_2(\mu\text{-H})_4]$ ($\text{M} = \text{Fe}, \text{Ru}$),⁴ $[\text{M}_2(\eta^6\text{-C}_6\text{Me}_6)_2(\mu\text{-H})_3]^+$ ($\text{M} = \text{Ru}, \text{Os}$),⁵ and $[\text{Mo}_2\text{Cp}_2(\mu\text{-H})(\mu\text{-PCy}_2)(\text{CO})_2]$.⁶ The high reactivity of these molecules under mild conditions can be used to synthesize heterometallic clusters by just reacting them with the appropriate metal complexes, often under the guidance of the isolobal analogies,⁷ as shown by the extensive work on the matter carried out on the dihydrides $[\text{Os}_3(\mu\text{-H})_2(\text{CO})_{10}]$,⁸ $[\text{Re}_2(\mu\text{-H})_2(\text{CO})_8]$,^{2,9} and $[\text{Mn}_2(\mu\text{-H})_2(\text{CO})_6(\mu\text{-L}_2)]$.¹⁰ However, among the available 30-electron hydride complexes, only the dimolybdenum one has been explored in that direction, even if these highly unsaturated substrates would seem more suitable for the incorporation of two, rather than one heterometal fragment. In particular, the reactions of the mentioned Mo_2 hydride with different metal carbonyl complexes of the types $[\text{M}_n(\text{CO})_m]$ and $[\text{M}_n(\text{CO})_m\text{Cp}_x]$ ($n =$

1, 2; $m = 4\text{--}10$) revealed two different pathways leading to heterometallic complexes: (a) formal replacement of the hydride ligand with a 17-electron metal fragment and (b) addition of a 16-electron metal fragment to give an hydride-bridged derivative.^{6c} In all cases, however, just one metal fragment was added to the dimolybdenum center, to give triangular unsaturated clusters (illustrated in Scheme 1 through the reactions with $[\text{W}(\text{CO})_6]$ and $[\text{W}_2\text{Cp}_2(\text{CO})_6]$).

Scheme 1

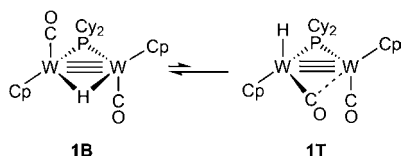


Received: March 11, 2013

Published: June 3, 2013

Recently, we reported the synthesis of the analogous unsaturated ditungsten hydride $[\text{W}_2\text{Cp}_2(\text{H})(\mu\text{-PCy}_2)(\text{CO})_2]$ (**1**).¹¹ A remarkable difference with its molybdenum analogue was the presence in solution of two isomers in equilibrium: a major one with a bridging hydride ligand (the unique isomer present in the molybdenum complex, **1B** in Chart 1) and a

Chart 1

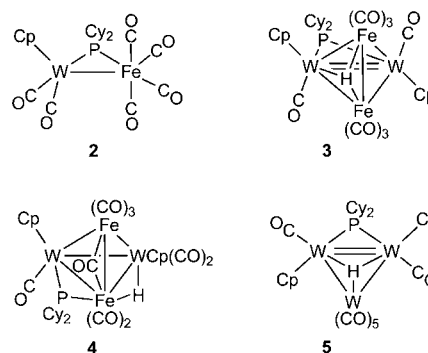


minor isomer with a terminal hydride and a semibridging carbonyl (**1T** in Chart 1). It could be anticipated that the presence of the isomer **T** in the solutions of **1** might imply a significant modification in the reactivity of this ditungsten complex; moreover, the replacement of molybdenum with tungsten in the 30-electron hydrides $[\text{M}_2\text{Cp}_2(\text{H})(\mu\text{-PCy}_2)(\text{CO})_2]$ should also have significant effects on the structure and stability of the corresponding derivatives. These differences might be particularly dramatic concerning the use of these hydrides as precursors of heterometallic clusters, where the different strengths of the Mo–M vs W–M bonds might make a great difference. Organometallic clusters have been a matter of interest for a long time, not only because of their structures and bonding, but also because of their potential use in homogeneous catalysis or in the synthesis of homo and heterometallic nanoparticles.¹² Moreover, heterometallic clusters can be used as models to get insight into the origins of the cooperative reactivity experimentally found in different heterogeneous mixed-metal catalysts.¹³ Yet, the implementation of rational synthetic procedures for heterometallic clusters remains a valuable target in this field. For these reasons, it was of interest to examine the potential of the ditungsten hydride **1** as a precursor of novel heterometallic derivatives, with special focus on the changes in structure and nuclearity derived from the presence of W instead of Mo at the unsaturated dimetal center of these complexes. In this paper, we report our studies on the reactions of the ditungsten hydride **1** with different transition-metal complexes to give heterometallic clusters. As it will be shown, the ditungsten **1** behaves differently from its dimolybdenum analogue and allows the formation of not only trinuclear but also tetranuclear heterometallic clusters with W_2M_2 metal cores, by following the reaction pathways outlined in Scheme 1. In addition, it can yield novel heterometallic clusters through a third reaction pathway, which involves the addition of unsaturated metal-hydride fragments to the ditungsten center.

RESULTS AND DISCUSSION

Reactions of 1 with Precursors of 16-Electron Metal Fragments. Compound **1** reacts with $[\text{Fe}_2(\text{CO})_9]$ (which is a classical precursor of the 16-electron $\text{Fe}(\text{CO})_4$ fragment) in tetrahydrofuran (THF) at room temperature to give a mixture of three new complexes: the heterodinuclear compound $[\text{FeWCp}(\mu\text{-PCy}_2)(\text{CO})_6]$ (**2**), and the tetranuclear clusters $[\text{Fe}_2\text{W}_2\text{Cp}_2(\mu_3\text{-H})(\mu\text{-PCy}_2)(\text{CO})_8]$ (**3**) and $[\text{Fe}_2\text{W}_2\text{Cp}_2(\mu\text{-H})(\mu\text{-PCy}_2)(\mu\text{-CO})(\text{CO})_8]$ (**4**), in a molar ratio of ca. 2.5:1:1, respectively (Chart 2). It is obvious that the formation of compound **2** requires cleavage of the W–W bond in **1** at

Chart 2



some stage, thereby constituting a decomposition pathway that competes with the formation of clusters **3** and **4**. On the other hand, it is likely that the reaction leading to the tetranuclear complexes takes place through the stepwise addition of $\text{Fe}(\text{CO})_4$ fragments to the hydride **1**, to give, first, a trinuclear W_2Fe intermediate that was not detected. Presumably this unstable species would partially degrade (W–W cleavage) to give **2**, or add a second $\text{Fe}(\text{CO})_4$ fragment to yield the unsaturated cluster **3** and the electron-precise **4**. We note that, although the latter compound has one more carbonyl than **3**, it is not a precursor of such an unsaturated cluster, since separate experiments revealed that compound **4** does not undergo spontaneous decarbonylation in solution at room temperature. Another experiment revealed that compound **3** does not react with CO (1 atm) in solution at room temperature. Therefore, we can safely conclude that compounds **3** and **4** are formed through different reaction pathways.

The photochemical reaction of the hydride **1** with $[\text{Ru}_3(\text{CO})_{12}]$ (a precursor of the $\text{Ru}(\text{CO})_4$ fragment under photochemical conditions), gave the binuclear complex $[\text{RuWCp}(\mu\text{-PCy}_2)(\text{CO})_6]$ as major product, along with other unidentified products. Although none of these compounds could be isolated nor properly characterized, the proposal of the RuW product as an analogue of compound **2** is strongly suggested by considering the similitude of its ^{31}P NMR resonance (δ_{P} 148.1 ppm, $J_{\text{PW}} = 304$ Hz) with that of **2** (Table 1).

The above results prove the strong influence that the metal in the unsaturated hydrides $[\text{M}_2\text{Cp}_2(\text{H})(\mu\text{-PCy}_2)(\text{CO})_2]$ exerts on the formation of heteronuclear derivatives: the dimolybdenum analogue of **1** reacted with $[\text{Fe}_2(\text{CO})_9]$ to give only a mixture of the binuclear products $[\text{FeMoCp}(\mu\text{-PCy}_2)(\text{CO})_6]$ and $[\text{Mo}_2\text{Cp}_2(\text{CO})_6]$, and a complex mixture of uncharacterized species were formed in the photochemical reaction with $[\text{Ru}_3(\text{CO})_{12}]$.^{6c} Therefore, it seems that the anticipated higher strength of the W–W and W–M bonds (vs Mo–Mo and Mo–M bonds) is indeed a critical factor enabling the formation of heterometallic clusters from these unsaturated hydrides.

The hydride **1** also reacted with the Group 6 metal carbonyls $[\text{M}(\text{CO})_6]$ (M = Cr, Mo, W) in toluene solution under ultraviolet–visible (UV–Vis). When M = Cr, Mo, however, no heterometallic cluster was detected in the reaction mixture, and the only P-containing species formed was the known tetracarbonyl complex $[\text{W}_2\text{Cp}_2(\mu\text{-H})(\mu\text{-PCy}_2)(\text{CO})_4]$,¹⁴ which obviously follows from the undesired reaction of **1** with the CO released in the photolysis of the hexacarbonyls $[\text{M}(\text{CO})_6]$. In contrast, the photolysis of mixtures of the hydride **1** and $[\text{W}(\text{CO})_6]$ in toluene led in a few minutes to a

Table 1. Selected IR^a and ³¹P{¹H}NMR^b Data for New Compounds

compound	$\nu(\text{CO})$	$\delta(\mu\text{-P}) [J_{\text{PW}}]$
[W ₂ Cp ₂ (H)(μ-PCy ₂)(CO) ₂] (1) ^c	1864 (w, sh), 1822 (vs)	167.2 [318] ^d
[FeWCp(μ-PCy ₂)(CO) ₆] (2)	2066 (s), 2012 (m), 1987 (vs), 1980 (s), 1928 (s), 1858 (s) ^e	147.6 [287] ^f
[Fe ₂ W ₂ Cp ₂ (μ ₃ -H)(μ-PCy ₂)(CO) ₈] (3)	2027 (s), 1984 (vs), 1958 (m), 1947 (m), 1937 (w), 1890 (vw, br), 1810 (w, br) ^g	121.8 [254] ^{f,h}
[Fe ₂ W ₂ Cp ₂ (μ-H)(μ-PCy ₂)(μ-CO)(CO) ₈] (4)	2022 (vs), 1986 (s), 1964 (s), 1948 (m), 1931 (w), 1913 (w), 1851 (m), 1772 (m) ^g	272.1 [262] ^{d,f}
[W ₃ Cp ₂ (μ ₃ -H)(μ-PCy ₂)(CO) ₇] (5)	2056 (m), 1970 (w, sh), 1934 (vs), 1902 (m, sh), 1840 (w)	125.5 [320, 320] ^h
[RuW ₂ Cp ₃ (μ-PCy ₂)(CO) ₄] (6)	1917 (m), 1893 (vs), 1815 (m), 1788 (w) ^g	183.1 [285] ⁱ
[Cu ₂ W ₂ Cp ₂ (μ-H) ₃ (μ-PCy ₂)(CO) ₂ (PPh ₃) ₂] (7)	1752 (m), 1869 (vs)	45.0 [240, 182] (isom M) ^f 31.6 [203, 203] (isom N) ^f

^aRecorded in dichloromethane (DCM) solution, with C–O stretching bands ($\nu(\text{CO})$) (given in units of cm^{-1} , unless otherwise stated). ^bRecorded in CD₂Cl₂ solutions at 290 K and 162.00 MHz, unless otherwise stated; δ in ppm relative to external 85% aqueous H₃PO₄, and J_{PW} in Hz. ^cData for the H-bridged isomer, taken from reference 11. ^dRecorded at 213 K. ^eIn petroleum ether solution. ^fIn C₆D₆ solution. ^gIn toluene solution. ^hRecorded at 121.49 MHz. ⁱRecorded at 233 K.

mixture of the 46-electron cluster [W₃Cp₂(μ₃-H)(μ-PCy₂)(CO)₇] (5), and the mentioned tetracarbonyl [W₂Cp₂(μ-H)(μ-PCy₂)(CO)₄]. Unfortunately, we could not suppress the formation of the latter species, derived from the efficient competition of CO (vs the W(CO)₅ fragment) for the unsaturated dimetal center of 1. In fact, the failure of 1 to give the W₂Mo or W₂Cr analogues of 5 is unlikely due to a particularly low stability of these putative molecules (expected to be more stable than the related Mo₃ and Mo₂Cr clusters actually obtained from the dimolybdenum analogue of 1),^{6c} and probably is just derived from the very fast carbonylation of the hydride 1, perhaps related, in turn, to the presence of isomers 1B and 1T in solution. We finally note that the tetracarbonyl [W₂Cp₂(μ-H)(μ-PCy₂)(CO)₄] was the only product formed in the room-temperature reaction of the THF solvate [Mn(η⁵-C₅H₄Me)(CO)₂(THF)] with 1, or upon photolysis of toluene solutions of 1 and [Mn(η⁵-C₅H₄Me)(CO)₃].

Solution Structure of Compound 2. Spectroscopic data in solution for 2 (Table 1 and Experimental Section) are very similar to those of the analogous molybdenum complex [FeMoCp(μ-PCy₂)(CO)₆], the structure of which was determined crystallographically; therefore, a similar structure is assumed for this FeW molecule (Chart 2). As expected, the IR spectrum in petroleum ether displays six C–O stretching bands (between 2066 and 1858 cm^{-1} , see Table 1), with a pattern similar to that measured for the mentioned FeMo complex or its PPh₂-bridged analogue [FeMoCp(μ-PPh₂)(CO)₆].¹⁵ The four bands at higher frequency are mainly due to the carbonyl ligands in the Fe(CO)₄ fragment and have frequencies virtually identical to those in the analogous FeMo complex as expected, while the two less-energetic bands are assigned to the W(CO)₂ oscillator and have frequencies almost identical to those of the tetracarbonyl hydride [W₂Cp₂(μ-H)(μ-PCy₂)(CO)₄]¹⁴ (also obtained as a minor product in this reaction). We finally note that the ³¹P NMR spectrum of 2 displays a resonance at 147.6 ppm, a chemical shift consistent the presence of a PR₂ ligand bridging W and Fe atoms (cf. 161 ppm in [Fe₂WCp(μ₃-η²-HCCPh)(μ-CO)(μ-PPh₂)(CO)₅]),¹⁶ with satellite lines corresponding to the coupling to a single ¹⁸³W nucleus ($J_{\text{PW}} = 287$ Hz).

Solid-State and Solution Structure of Compound 3. The molecule of 3 in the crystal (Figure 1 and Table 2) displays a tetrahedral metal core that can be viewed as built from a transoid W₂Cp₂(μ-PCy₂)(CO)₂ fragment perpendicularly bound to a Fe₂(CO)₆ moiety. The unsaturation of the Fe(CO)₃ fragments is mitigated with a weak semibringing

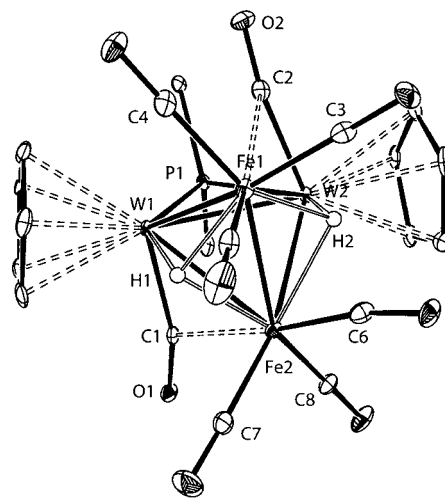


Figure 1. ORTEP diagram (30% probability) of compound 3, with Cy groups (except their C¹ atoms) and H atoms (except the hydride ligand, 50% disordered over the positions H1 and H2) omitted for clarity.

Table 2. Selected Bond Lengths and Bond Angles for 3

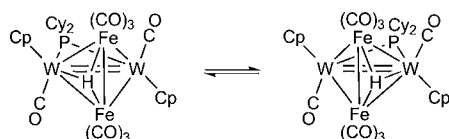
bond lengths (Å)		bond angles (deg)	
W1–W2	2.704(1)	W1–P1–W2	68.4(2)
W1–Fe1	2.834(1)	W2–Fe2–H1	87.0(5)
W1–Fe2	2.812(1)	Fe1–Fe2–H1	45.0(5)
W2–Fe1	2.867(1)	W1–Fe2–H1	41.0(6)
W2–Fe2	2.661(1)	W1–C1–O1	162.1(6)
Fe1–Fe2	2.553(1)	Fe2–W1–C1	58.0(2)
W1–P1	2.407(2)	W1–C1–Fe2	78.5(2)
W2–P1	2.403(2)	W2–C2–O2	166.0(6)
W1–H1	1.9(2)	Fe1–Fe2–W1	63.5(1)
Fe1–H1	1.8(2)	Fe1–Fe2–W2	66.7(1)
Fe2–H1	1.8(2)	Fe2–C6–O6	167.5(6)
Fe1–C3	1.780(8)		
Fe2–C6	1.767(7)		
W1–C1	1.974(7)		
W2–C2	1.965(8)		

interaction from the W-bound carbonyls (Fe1...C2, ca. 2.60 Å; Fe2...C1, ca. 2.44 Å) and by the presence of a face-bridging hydride ligand, found to be disordered over both WF₂ faces. Overall, compound 3 has 58 cluster valence electrons (CVE)—hence, two electrons below the required number for an electron-precise tetrahedral core—and this unsaturation seems

to be mainly located at the ditungsten center. Thus, the W–Fe lengths (in the range of 2.66–2.87 Å) and the Fe1–Fe2 separation of 2.553(1) Å are marginally shorter or similar to the single bonds between these metal atoms in the electron-precise cluster 4 (W–Fe in the range 2.78–2.90 Å; Fe–Fe = 2.545(2) Å, see below). In contrast, the W1–W2 separation of 2.704(1) Å is notably shorter than common single-bond lengths (above ca. 2.9 Å), even shorter than the intermetallic separation in the 32-electron diphosphine-bridged complex $[\text{W}_2\text{Cp}_2(\mu\text{-COMe})(\text{CO})_2(\mu\text{-Ph}_2\text{PCH}_2\text{PPh}_2)]^+$ (2.781(3) Å), a cation having a W–W double bond.¹⁷ A similar localization effect has been observed recently for related unsaturated molybdenum clusters, also displaying short Mo–Mo bonds, such as the 46-electron clusters $[\text{Mo}_3\text{Cp}_3(\mu\text{-PCy}_2)(\mu_3\text{-CO})(\text{CO})_4]$ (2.743(1) Å),^{6c} and $[\text{Mo}_2\text{RuCp}_2(\mu_3\text{-CH})(\mu\text{-PCy}_2)(\text{CO})_5]$ (2.6824(7) Å),¹⁸ or the 58-electron tetrahedral species $[\text{Co}_2\text{Mo}_2\text{Cp}_2(\mu_3\text{-COMe})(\mu\text{-PCy}_2)(\mu\text{-CO})_2(\text{CO})_4]$ (2.6857(6) Å).¹⁹ As for related clusters having tetrahedral W_2M_2 cores, we note that only a few involving Group 8 metals have been structurally characterized so far,^{20–22} and all of them are 60-CVE species, with the exception of the imido-bridged W_2Ru_2 cluster $[\text{W}_2\text{Ru}_2(\mu\text{-NPh})(\mu_3\text{-HC}_2\text{Ph})(\text{CO})_6]$,^{21a} which displays an even shorter W–W separation of 2.592 Å, in part due to the small-sized N atom (compared to P) actually bridging the W–W edge of the tetrahedron.

Spectroscopic data for 3 in solution are essentially consistent with the structure found in the solid state. The IR spectrum in toluene solution displays two bands around 2000 cm^{-1} consistent with the presence of a $[\text{Fe}(\text{CO})_3]_2$ oscillator in the molecule,²³ although the bands mainly arising from the transoid $\text{W}_2(\text{CO})_2$ oscillator are better appreciated in the solid-state IR spectra, which displays two bands at 1876 and 1811 cm^{-1} with weak and medium intensities, respectively. The ³¹P NMR spectrum displays a single resonance at 121.8 ppm, a chemical shift some 50 ppm below the resonances measured in the unsaturated molybdenum clusters mentioned above,^{6c,18,19} as expected from the change in metals; however, this resonance displays identical couplings to both W atoms (254 Hz). Consistent with the latter observation, the ¹H NMR spectrum of 3 displays just a single resonance for the cyclopentadienyl groups, while the hydride ligand gives rise to a resonance at –13.16 ppm, with identical couplings to the inequivalent W atoms (31 Hz). All of this reveals the occurrence in solution of a dynamic process, fast on the NMR time scale, whereby the hydride ligand exchanges its position between both Fe_2W faces (thus reproducing the disorder found in the crystal), therefore rendering equivalent $\text{WCp}(\text{CO})$ fragments (Scheme 2). Low-

Scheme 2. Fluxional Process Proposed for Compound 3 in Solution



temperature NMR measurements confirmed this hypothesis. Thus, upon cooling a toluene-*d*₈ solution of 3, the unique Cp resonance at 5.11 ppm broadened and eventually split into two resonances of the same intensity below 229 K (coalescence temperature), to give sharp lines at 4.94 and 4.80 ppm at 193 K. From these data, we can estimate a Gibbs free energy of

activation of 46.5 ± 1 kJ/mol for the corresponding process.²⁴ As expected, the satellite lines of the hydride resonance were also affected by the temperature: they showed a progressive broadening from 293 K to ca. 230 K and then a progressive sharpening on further cooling. Below 213 K, the hydride resonance displayed a pair of broad satellites (J_{PW} ca. 56 Hz) with intensity denoting coupling to a single ¹⁸³W nucleus. From this and the average coupling of 31 Hz, we can estimate a coupling of ca. 4 Hz to the second W atom (obviously hidden under the central line of the resonance), which is consistent with the static structure of the cluster, with a hydride ligand directly bound to just one W atom.

Solid-State and Solution Structure of Compound 4. The molecule of 4 in the crystal (Figure 2 and Table 3) also

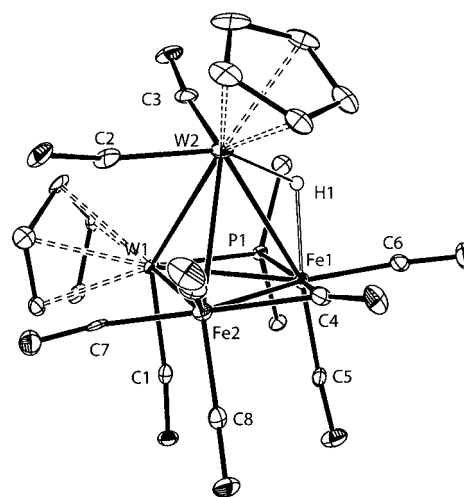


Figure 2. ORTEP diagram (30% probability) of compound 4, with Cy groups (except their C¹ atoms) and H atoms (except the hydride ligand) omitted for clarity.

displays a tetrahedral W_2Fe_2 core, but now there is one more carbonyl ligand, thus yielding an electron-precise 60-CVE cluster. In agreement with this, all intermetallic separations fall within the range expected for the corresponding single metal–metal bonds. In particular, the W–W separation of 3.058(5) Å

Table 3. Selected Bond Lengths and Bond Angles for 4

bond lengths (Å)		bond angles (deg)	
W1–W2	3.058(5)	W1–P1–Fe1	73.3(1)
W1–Fe1	2.778(1)	C1–W1–P1	86.9(2)
W1–Fe2	2.805(1)	W1–C1–O1	174.6(6)
W2–Fe1	2.900(1)	Fe1–C4–O4	140.0(7)
W2–Fe2	2.804(1)	Fe2–C4–O4	139.1(7)
Fe1–Fe2	2.545(2)	Fe1–C4–Fe2	80.8(3)
W1–P1	2.403(2)	C4–Fe2–C9	89.2(4)
Fe1–P1	2.246(2)	C4–Fe2–C7	176.7(4)
W2–H1	1.80(7)	C4–Fe2–C8	89.1(3)
Fe1–H1	1.71(7)	C4–Fe1–H1	94(2)
Fe1–C4	1.944(9)	C4–Fe1–P1	167.3(2)
Fe2–C4	1.981(8)	C5–Fe1–P1	95.8(3)
W2–C2	2.000(9)	C6–Fe1–P1	100.1(3)
Fe1–C5	1.769(8)	H1–Fe1–P1	80(2)
Fe2–C8	1.781(8)	H1–Fe1–C5	170(2)
W1–C1	1.960(8)		
W2–C2	2.000(9)		

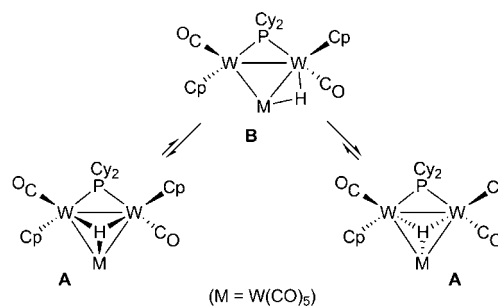
is 0.3 Å larger than the corresponding length in **3**, and it can be now identified with the presence of a single W–W bond. The arrangement of ligands around the tetrahedral core, however, is quite different from that in **3**. The molecule can be viewed as built from WCp(CO), Fe(CO)₃, and Fe(CO)₂ fragments defining a triangle and symmetrically bridged, almost in the same plane, by a carbonyl and the PCy₂ ligand, on Fe–Fe and W–Fe edges, respectively, with a further WCp(CO)₂ fragment as the fourth corner of the tetrahedron and the hydride ligand placed over the bond between the latter and the Fe(CO)₂ fragment. As expected, this bond is elongated (by ca. 0.1 Å) with respect to the other W–Fe bond involving the same W fragment. We should note that, among all tetrahedral clusters with M₂M'₂ cores combining metal atoms of the Groups 6 and 8 that have been crystallographically characterized so far, only one of them ([Fe₂Mo₂Cp₂(μ-Sph)(μ₃-S)(μ₃-Te)(μ₃-H)(μ-CO)(CO)₄]) bears hydride ligands, actually bridging a Fe₂Mo face.²⁵

The spectroscopic data in solution for compound **4** are in good agreement with the structure found in the crystal. The IR spectrum in the C–O stretching region is quite complex, as expected from the high number of carbonyl ligands and low symmetry of the cluster, and the less energetic band at 1772 cm⁻¹ can be safely assigned to the carbonyl group bridging the Fe–Fe edge of the molecule. The phosphide ligand gives rise to a ³¹P NMR resonance displaying coupling to a single W nucleus (*J*_{PW} = 262 Hz), as expected for a ligand bridging a W–Fe edge. However, its strong deshielding (*δ*_p 272.1 ppm) cannot be due just to the influence of the metal atoms involved (W and Fe). In fact, different WFe₂ clusters with PR₂ ligands bridging Fe–W edges give rise to resonances less deshielded, all below 200 ppm.^{16,26} Instead, the strong ³¹P deshielding in **4** rather seems to constitute another example of the so-called cluster effect, an empirical correlation between the chemical shift of a PR₂ ligand and the nuclearity of the cluster to which it is bound, that seems to be related with the progressive reduction in the HOMO/LUMO gap of clusters upon increasing its nuclearity.²⁷ We have previously observed a strong deshielding effect in the 60-electron cluster [Co₂Mo₂Cp₂(μ₃-COMe)(μ-PCy₂)(μ-CO)(CO)₆], which displays a ³¹P resonance at 340.5 ppm for the PCy₂ group bridging one of the Mo–Co edges of the molecule.¹⁹ As for the ¹H NMR resonances, we note that the inequivalent Cp ligands give rise to separate resonances as expected, while the hydride ligand renders a resonance at –20.74 ppm, a position notably more shielded than those of H ligands bridging two W atoms (cf. –16.4 ppm in [W₂Cp₂(μ-H)(μ-PCy₂)(CO)₄]),¹⁴ and displaying coupling to a single ¹⁸³W nucleus, all of this being consistent with its positioning between W and Fe atoms, as found in the crystal. We also note that the latter coupling is comparable to the one measured for **3** (53 vs 58 Hz), despite the different coordination environments of the corresponding hydride ligands (μ₂ vs μ₃).²⁸

Solution Structure of Compound 5. The spectroscopic data available for compound **5** (Table 1 and Experimental Section) are comparable to those of [WMo₂Cp₂(μ₃-H)(μ-PCy₂)(CO)₇], a molecule generated through the photochemical reaction of W(CO)₆ with the Mo₂ analogue of **1** and characterized through an X-ray study (Scheme 1).^{6c} Therefore, a similar structure is assumed for **5**, derived from the addition of a W(CO)₅ fragment to the unsaturated W₂(μ-H) center of **1** (Chart 2). The presence of the latter carbonyl fragment is denoted by the appearance in the IR spectrum of **5** of a band at 2056 cm⁻¹, a position characteristic of the

symmetric C–O stretch in pentacarbonyl complexes of the type M(CO)₅L (M = Cr, Mo, W).²³ The hydride ligand gives rise to a ¹H NMR resonance at –7.78 ppm, not far from that of the parent hydride **1**,¹¹ and displays coupling to the ¹⁸³W nucleus of the W(CO)₅ fragment (*J*_{HW} = 32 Hz) and to both nuclei of the WCp(CO) fragments (*J*_{HW} = 84 Hz), in agreement with its μ₃-coordination. However, both the degeneracy of the latter coupling, and the appearance of a single resonance for the cyclopentadienyl groups of the molecule, are inconsistent with the proposed structure having transoid and inequivalent WCp(CO) fragments. This circumstance was also found for the Mo₂W analogue of compound **5**, and it was explained at the time by assuming a dynamic process in solution whereby the hydride ligand moves from one side to the other of the metal triangle, thus creating in the fast exchange limit an apparent C₂ symmetry axis bisecting the Mo₂W core, although no proof of it was given. In the case of **5**, the corresponding dynamic process seems to be rather slow, since its room temperature ¹³C NMR spectrum displays separated resonances for the inequivalent Cp and Cy pairs, and only the appearance of a single resonance for the inequivalent carbonyls of the W₂Cp₂ fragment (*δ* 231.6 ppm) denotes the operation of a dynamic process (see the Experimental Section). Indeed, this resonance split into two resonances (*δ* 234.5 and 234.3 ppm) at 213 K. Unfortunately, low-temperature ¹H and ³¹P NMR measurements failed to detect the expected splitting in the Cp resonances or in the satellite lines of the hydride and phosphide resonances (only a progressive broadening of these resonances was observed), perhaps due to the close values of the corresponding parameters in the static structure. Interestingly, however, a splitting of the overall phosphide and hydride resonances was observed at very low temperatures, below ca. 193 K (P) or 173 K (H), to give in each case two separate and broad resonances in a ca. 1:4 ratio (see the Experimental Section). This reveals the presence in solution of two rapidly exchanging isomers of **5**, which we propose to differ essentially in the position of the bridging hydride, either placed over the W₃ triangle (**A**, the one found in the crystal) or bridging a W₂ edge (**B** in Scheme 3).

Scheme 3. Dynamic Process Proposed for Compound 5 in Solution



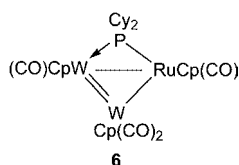
The equilibrium between these isomers obviously allow for the overall shift of the hydride ligand from one side to the other of the W₃ plane, thus accounting for the observed averaging of NMR parameters at room temperature.

Reactions of 1 with Precursors of 17-Electron Metal Fragments. We have examined the reactions of **1** with several simple metal–metal bonded compounds such as the cyclopentadienyl dimers [M₂Cp₂(CO)_n] (M = Mo, W, n = 6; M = Fe, Ru, n = 4) and the carbonyl dimers [M₂(CO)_n] (M = Mn, n = 10; M = Co, n = 8). Except for the cobalt complex, no

reaction occurred unless the solutions were irradiated with visible-UV light, presumably because this triggers the homolytic fission of the metal–metal bond in the dimers to generate very reactive 17-electron radicals, a process typically competing with photodissociation of CO.²⁹

No heterometallic cluster was formed upon photolysis of mixtures **1** and $[\text{Fe}_2\text{Cp}_2(\text{CO})_4]$, which yielded instead the tetracarbonyl complex $[\text{W}_2\text{Cp}_2(\mu\text{-H})(\mu\text{-PCy}_2)(\text{CO})_4]$, obviously formed through the reaction of **1** with photogenerated CO. In contrast, UV-Vis irradiation of toluene solutions of equimolar mixtures of **1** and $[\text{Ru}_2\text{Cp}_2(\text{CO})_4]$ at 263 K gave the heterometallic cluster $[\text{RuW}_2\text{Cp}_3(\mu\text{-PCy}_2)(\text{CO})_4]$ (**6**) (Chart 3) in only 5 min. This parallels the behavior of the Mo₂

Chart 3



analogue of **1** to yield a related cluster $[\text{RuMo}_2\text{Cp}_3(\mu\text{-PCy}_2)(\text{CO})_4]$ which, however, displayed an equilibrium mixture of two isomers differing in the position of the PCy₂ bridge on the Mo₂Ru metal skeleton.^{6c} In contrast, the tungsten cluster **6** is formed as a single isomer, specifically with the PCy₂ ligand bridging a W–Ru edge.

Although we could not obtain suitable crystals of this complex for a crystallographic study, the available spectroscopic data allow us to define the major structural features of the molecule. This tetracarbonyl species displays four C–O stretching bands ranging from 1917 cm⁻¹ to 1788 cm⁻¹ in its IR spectrum and four distinct carbonyl resonances ranging from 231 ppm to 206 ppm in the ¹³C NMR spectrum, this supporting the presence of essentially terminal carbonyls over a trimetal core lacking any symmetry element. In agreement with this, the ¹H NMR spectrum displays three distinct resonances for the cyclopentadienyl groups of the molecule. As for the ³¹P NMR spectra, compound **6** gives rise to a single resonance at 183.1 ppm displaying coupling to a single ¹⁸³W nucleus (*J*_{WP} = 285 Hz), therefore identifying its position as a bridging group over a W–Ru edge of the cluster. The only undefined structural feature of the molecule is the relative conformation of the MCp(CO)_x fragments, with respect to the W₂Ru plane, since four different conformers are theoretically possible in this case.

We have previously shown that the molybdenum analogue of **1** is able to react with the radicals formed upon visible-light irradiation of the dimers $[\text{M}_2\text{Cp}_2(\text{CO})_6]$ (M = Mo, W) to form trinuclear clusters and HMCp(CO)₃ (Scheme 1).^{6c} Unfortunately, the reactions of **1** with these dimers under the same conditions yielded the tetracarbonyl $[\text{W}_2\text{Cp}_2(\mu\text{-H})(\mu\text{-PCy}_2)(\text{CO})_4]$ as major product, along with small amounts of the mononuclear hydrides $[\text{HMCp}(\text{CO})_3]$. This can be justified by taking into consideration that the greater strength of the W–H bonds (compared to Mo–H ones) would make the hydride abstraction from **1** by the $[\text{MCp}(\text{CO})_3]$ radicals a more-difficult process, this eventually imposing a higher barrier to the formation of heterometallic clusters. Instead, the $[\text{MCp}(\text{CO})_3]$ radicals would rather decompose progressively, then releasing CO which reacts with **1** rapidly to form the ubiquitous tetracarbonyl hydride product. A similar explanation can be given to account for the fact that the photolysis of **1** and

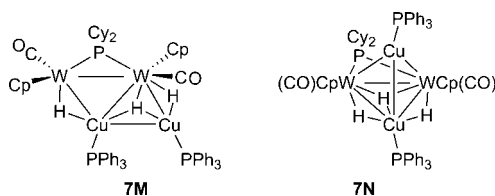
$[\text{Mn}_2(\text{CO})_{10}]$ gave the hydride $[\text{W}_2\text{Cp}_2(\mu\text{-H})(\mu\text{-PCy}_2)(\text{CO})_4]$ once more as major product.

The hydride **1** turned to be very reactive toward $[\text{Co}_2(\text{CO})_8]$ in the absence of light. Unfortunately, this reaction takes place rapidly in toluene solution, even at 253 K, to give a mixture of products that could not be isolated nor properly characterized, with the tetracarbonyl complex $[\text{W}_2\text{Cp}_2(\mu\text{-H})(\mu\text{-PCy}_2)(\text{CO})_4]$ being present in substantial amounts once more.

Reaction of 1 with $[\text{Cu}(\text{BH}_4)(\text{PPh}_3)_2]$. We have shown previously that the tetrahydroborate copper complex $[\text{Cu}(\text{BH}_4)(\text{PPh}_3)_2]$ behaves as a source of the hydride fragment $[\text{CuH}(\text{PPh}_3)]$ when reacting with the unsaturated dihydride $[\text{Mn}_2(\mu\text{-H})_2(\text{CO})_6(\mu\text{-tedip})]$ (tedip = (EtO)₂POP(OEt)₂), to give the trimetallic cluster $[\text{CuMn}_2(\mu\text{-H})_3(\text{CO})_6(\mu\text{-tedip})\text{-}(\text{PPh}_3)]$ with concomitant formation of $\text{BH}_3\cdot\text{PPh}_3$.^{10c} Thus, it was thought that the hydride **1** should be able to undergo a similar reaction thereby incorporating one or perhaps two copper fragments, with the latter yielding a more-saturated derivative. Indeed, **1** reacts with 2 equiv of $[\text{Cu}(\text{BH}_4)(\text{PPh}_3)_2]$ slowly at room temperature (reaction completed in ca. 24 h) to give the tetranuclear cluster $[\text{Cu}_2\text{W}_2\text{Cp}_2(\mu\text{-H})_3(\mu\text{-PCy}_2)(\text{CO})_2(\text{PPh}_3)_2]$ (**7**), along with the adduct $\text{BH}_3\cdot\text{PPh}_3$, the latter being identified through its characteristic ³¹P NMR resonance. Noticeably, the same result was obtained when using stoichiometric amounts of reagents (of course, unreacted hydride **1** then remained in the solution). Moreover, a ³¹P NMR monitoring of this slow reaction failed to detect significant amounts of intermediate species. Therefore, we conclude that the putative trinuclear cluster $[\text{CuW}_2\text{Cp}_2(\mu\text{-H})_2(\mu\text{-PCy}_2)(\text{CO})_2(\text{PPh}_3)]$ following from the insertion of the first HCu(PPh₃) fragment is more reactive toward the tetrahydroborate complex than the hydride **1**, then it reacts preferentially with the copper reagent to yield the tetranuclear cluster **7**.

The NMR data for **7** (Table 1 and Experimental Section) indicate that this species exists in solution as an equilibrium mixture of two isomers **M** and **N**, in a ratio **M/N** of ca. 10 in C₆D₆ solution (Chart 4). The IR spectrum in petroleum ether

Chart 4



displays three C–O stretching bands, with those at 1772 cm⁻¹ (m) and 1721 cm⁻¹ (vs) being assigned to the major isomer **M**. The relative intensities of these bands indicates the retention of the transoid arrangement of the WCp(CO) fragments found in the parent hydride **1**, and possibly this also applies to the minor isomer **N**. The ³¹P NMR spectrum of the major isomer is indicative of an asymmetric structure, with the phosphide ligand coupled to inequivalent ¹⁸³W nuclei (*J*_{WP} = 240 and 182 Hz) and inequivalent copper-bound P atoms (δ_p 15.5 and 13.3 ppm). The minor isomer also displays inequivalent copper-bound P atoms (δ_p 15.1 and 13.3 ppm) but the W atoms now seem to be equivalent, since the phosphide resonance displays identical couplings of 203 Hz to both ¹⁸³W nuclei. The ¹H NMR data confirm the above conclusions and add further information concerning the positions of the three hydride

ligands present in each isomer. The chemical shifts for all these nuclei are found in the range of -8.4 ppm to -12.7 ppm, and are similar to those measured in the Cu–Mn clusters $[\text{Mn}_2\text{Cu}(\mu\text{-H})_3(\text{CO})_6(\text{PPh}_3)(\mu\text{-tedip})]$ and $[\text{Mn}_4\text{Cu}_2(\mu\text{-H})_6(\text{CO})_{12}(\mu\text{-tedip})_2]$ for the hydride ligands bridging Mn–Cu edges or Mn_2Cu and Cu_2Mn faces.^{10c} Therefore, the hydride ligands in both isomers of **7** are proposed to bridge either W–Cu edges or W_2Cu and Cu_2W faces. The three hydride resonances of the major isomer (-8.40 , -9.28 , and -9.60 ppm) display couplings to a single ^{183}W nucleus in each case, which is consistent with bridging positions over W–Cu edges or a WCu_2 face. This can be easily accomplished in a structure with a rhombus-shaped metal core (Chart 4), inspired in the structure of the mentioned Mn_4Cu_2 cluster, although alternative structures are possible. In contrast, the minor isomer displays just two hydride resonances with 2:1 intensities, a circumstance which can be justified with a structure based on a tetrahedral W_2Cu_2 core comparable to the one crystallographically characterized for the digold cluster $[\text{Au}_2\text{Mo}_2\text{Cp}_2(\mu\text{-PCy}_2)(\text{CO})_2(\text{P}^i\text{Pr}_3)_2]^+$,³⁰ but now with a hydride ligand bridging one of the W_2Cu faces and a pair of equivalent hydrides bridging either W–Cu edges or both WCu_2 faces. Unfortunately, all our attempts to grow single crystals of any of these isomers, to confirm the above proposals were unsuccessful. We note, in any case, that skeletal isomerism is a common circumstance found in the chemistry of heterometallic clusters of the transition elements and the coinage metals.³¹

CONCLUSION

The tungsten hydride **1** displays significant reactivity toward different mononuclear and binuclear transition-metal carbonyl complexes as well as a low-valency species of copper, to give distinct trinuclear and tetranuclear heterometallic clusters via three different reaction pathways. First, complex **1** can behave as a neat electron donor by using electron density accumulated at the $\text{W}_2(\mu\text{-H})$ region, thus forming the corresponding heterometallic cluster by coordination of **1** to a 16-electron metal fragment (which behaves as the electron acceptor), with this resulting in a heterometallic cluster with a $\text{W}_2\text{M}(\mu_3\text{-H})$ central core. The latter species can even add a further 16-electron fragment ($\text{M} = \text{Fe}$) to give a tetranuclear cluster with a $\text{W}_2\text{M}_2(\mu_3\text{-H})$ skeleton, a circumstance not observed for the dimolybdenum analogue of **1**. A second reaction pathway appears in the presence of 17-electron metal fragments, this involving the formal replacement of the hydride ligand of **1** with the radical fragment to give trinuclear clusters with a W_2M skeleton, only observed for $\text{M} = \text{RuCp}(\text{CO})_2$. This pathway seems particularly disfavored for **1**, possibly because of the higher strength of the W–H bond (compared to the Mo–H bond in its dimolybdenum analogue). The third reaction pathway involves the formal insertion of an unsaturated hydride metal fragment HML_n in the W–H bond of **1**, to give heterometallic clusters with W_2MH_2 or $\text{W}_2\text{M}_2\text{H}_3$ metal cores, and is the overall process that occurred in the reaction of **1** with $[\text{Cu}(\text{BH}_4)(\text{PPh}_3)_2]$ to give the tetranuclear cluster $[\text{Cu}_2\text{W}_2\text{Cp}_2(\mu\text{-H})_3(\mu\text{-PCy}_2)(\text{CO})_2(\text{PPh}_3)_2]$. This third pathway has not been reported for the dimolybdenum analogue of **1** so far.

EXPERIMENTAL SECTION

General Procedures and Starting Materials. All manipulations and reactions were carried out under a nitrogen (99.995%)

Table 4. Crystal Data for New Compounds

compound	Value	
	3	4
mol formula	$\text{C}_{30}\text{H}_{33}\text{Fe}_2\text{O}_8\text{PW}_2$	$\text{C}_3\text{H}_3\text{Fe}_2\text{O}_9\text{PW}_2$
mol wt	1031.93	1059.94
cryst syst	monoclinic	monoclinic
space group	$P2_1$	$P2_1/c$
radiation (λ)	0.71073 Å	0.71073 Å
unit-cell parameters		
<i>a</i>	9.3139(3) Å	9.2955(5) Å
<i>b</i>	16.3035(5) Å	16.2208(7) Å
<i>c</i>	10.4467(3) Å	21.1179(11) Å
α	90°	90°
β	103.507(2)	90.212(2)
γ	90°	90
<i>V</i>	1542.45(8) Å ³	3184.1(3) Å ³
<i>Z</i>	2	4
calcd density	2.222 g cm ⁻³	2.211 g cm ⁻³
absorption coefficient	8.456 mm ⁻¹	8.198 mm ⁻¹
temperature	100(2) K	100(2) K
θ range	2.25°–28.34°	1.58°–26.44°
index ranges (<i>h</i> , <i>k</i> , <i>l</i>)	<i>h</i> = $-12, 12$; <i>k</i> = $-21, 21$; <i>l</i> = $0, 13$	<i>h</i> = $-11, 11$; <i>k</i> = $0, 20$; <i>l</i> = $0, 26$
no. of reflns collected	28830	41478
no. of indep reflns (R_{int})	7595 (0.0352)	6562 (0.0829)
reflns with $I > 2\sigma(I)$	7371	4624
<i>R</i> indexes (data with $I > 2\sigma(I)$) ^a		
<i>R</i> ₁	0.0285	0.0380
<i>wR</i> ₂	0.0668 ^b	0.0611 ^c
<i>R</i> indexes (all data) ^a		
<i>R</i> ₁	0.0300	0.0774
<i>wR</i> ₂	0.0676 ^b	0.0715 ^c
goodness of fit, GOF	1.028	1.026
no. of restraints/parameters	16/391	42/406
$\Delta\rho(\text{max, min})$	0.611, $-0.943 \text{ e } \text{Å}^{-3}$	2.442, $-1.998 \text{ e } \text{Å}^{-3}$

^a $R_1 = \sum ||F_o| - |F_c|| / \sum |F_o|$. $wR_2 = [\sum w(|F_o|^2 - |F_c|^2)^2 / \sum w|F_o|^2]^{1/2}$. $w = 1/[\sigma^2(\sum F_o^2) + (aP)^2 + bP]$, where $P = (F_o^2 + 2F_c^2)/3$. ^b $a = 0.0284$, $b = 11.0318$. ^c $a = 0.0167$, $b = 19.6710$.

atmosphere using standard Schlenk techniques. Solvents were purified according to literature procedures and distilled prior to use.³² Compounds **1**,¹¹ $[\text{Mn}(\eta^5\text{-C}_5\text{H}_4\text{Me})(\text{CO})_2(\text{THF})]$,³³ $[\text{Ru}_2\text{Cp}_2(\text{CO})_4]$,³⁴ and $[\text{Cu}(\text{BH}_4)(\text{PPh}_3)_2]$,³⁵ were prepared according to literature procedures, and all other reagents were obtained from the usual commercial suppliers and used as received. Petroleum ether refers to that fraction distilling in the range of 338–343 K. Photochemical experiments were performed using jacketed quartz or Pyrex Schlenk tubes, cooled by tap water (ca. 288 K). A 400 W mercury lamp (as source of visible-UV light) or a conventional 200 W lamp (as source of visible light), both placed ca. 1 cm away from the Schlenk tube, were used for all the experiments. Chromatographic separations were carried out using jacketed columns cooled by tap water (ca. 288 K) or by a closed 2-propanol circuit, kept at the desired temperature with a cryostat. Commercial aluminum oxide (activity I, 150 mesh) was degassed under vacuum prior to use. The latter was afterward mixed under nitrogen with the appropriate amount of water to reach the activity desired. Filtrations were performed using diatomaceous earth. Infrared (IR) C–O stretching frequencies were measured in solution or Nujol mulls, are referred to as ν_{CO} (solvent) or ν_{CO} (Nujol), respectively, and are given in wavenumber units (cm⁻¹). Nuclear magnetic resonance (NMR) spectra were routinely recorded at 400.13 MHz (¹H), 162.00 MHz (³¹P{¹H}), or 100.62

MHz ($^{13}\text{C}\{^1\text{H}\}$) at 290 K in CD_2Cl_2 solutions, unless otherwise stated. Chemical shifts (δ) are given in ppm, relative to internal tetramethylsilane (^1H , ^{13}C) or external 85% aqueous H_3PO_4 solution (^{31}P). Coupling constants (J) are given in hertz (Hz).

Reaction of Compound 1 with $[\text{Fe}_2(\text{CO})_9]$. Solid $[\text{Fe}_2(\text{CO})_9]$ (0.024 g, 0.066 mmol) was added to a solution of complex 1 (0.050 g, 0.066 mmol) in THF (8 mL), and the mixture was stirred at room temperature for 15 min. A further amount of $[\text{Fe}_2(\text{CO})_9]$ (0.024 g, 0.066 mmol) then was added and the mixture was stirred at room temperature for 30 min to give an orange solution containing a mixture of the heterodinuclear compound $[\text{FeW}_2\text{Cp}_2(\mu\text{-PCy}_2)(\text{CO})_6]$ (2) and the heterometallic clusters $[\text{Fe}_2\text{W}_2\text{Cp}_2(\mu_3\text{-H})(\mu\text{-PCy}_2)(\text{CO})_8]$ (3) and $[\text{Fe}_2\text{W}_2\text{Cp}_2(\mu\text{-H})(\mu\text{-PCy}_2)(\mu\text{-CO})(\text{CO})_8]$ (4), in a ratio of ca. 2.5:1:1 (by NMR). The solvent was then removed under vacuum, the residue was extracted with dichloromethane (3 \times 6 mL), and the extracts were filtered. The solvent was then removed from the filtrate, and the residue was dissolved in the minimum amount of dichloromethane and chromatographed on alumina (activity II) at 253 K. Elution with dichloromethane/petroleum ether (1/4) gave an orange fraction containing compound 2 contaminated with small amounts of $[\text{W}_2\text{Cp}_2(\mu\text{-H})(\mu\text{-PCy}_2)(\text{CO})_4]$, which was not further purified. Elution with dichloromethane/petroleum ether (1/1) first gave a green fraction and then a brown fraction which yielded, respectively, after removal of solvents, compounds 3 (0.014 g, 20%) and 4 (0.014 g, 20%) as microcrystalline solids. The crystals used in the X-ray diffraction (XRD) studies were grown by the slow diffusion of a layer of petroleum ether into a dichloromethane solution of each of these complexes at 253 K.

Data for Compound 2. ^1H NMR (C_6D_6): δ 4.80 (s, 5H, Cp), 2.50–1.00 (m, 22H, Cy).

Data for Compound 3. Anal. Calcd for $\text{C}_{30}\text{H}_{33}\text{Fe}_2\text{O}_8\text{PW}_2$: C, 34.92; H, 3.22. Found: C, 34.70; H, 3.11. ν_{CO} (Nujol): 2019 (vs), 1981 (s), 1973 (s), 1955 (m), 1940 (s), 1919 (s), 1876 (w), 1811 (w). ^1H NMR (C_6D_6): δ 5.11 (s, 10H, Cp), 2.50–0.50 (m, 22H, Cy), –13.16 (d, $J_{\text{HP}} = 5$, $J_{\text{HW}} = 30$, 1H, $\mu_3\text{-H}$). ^1H NMR (toluene- d_8 , 298 K): δ 5.10 (s, 10H, Cp), 2.50–1.10 (m, 22H, Cy), –13.81 (d, $J_{\text{HP}} = 5$, $J_{\text{HW}} = 31$, 1H, $\mu_3\text{-H}$). ^1H NMR (toluene- d_8 , 229 K): δ 4.96 (s, br, 10H, Cp), –13.81 (d, $J_{\text{HP}} = 5$, with very broad W satellite lines, 1H, $\mu_3\text{-H}$). ^1H NMR (toluene- d_8 , 193 K): δ 4.94, 4.80 (2s, 2 \times 5H, Cp), –13.81 (d, br, $J_{\text{HP}} = 4$, with broad W satellite lines, $J_{\text{HW}} = 58$, 1H, $\mu_3\text{-H}$). $^{31}\text{P}\{^1\text{H}\}$ NMR (toluene- d_8 , 243 K): δ 121.7 (s, $J_{\text{PW}} = 254$). $^{31}\text{P}\{^1\text{H}\}$ NMR (toluene- d_8 , 208 K): δ 122.1 (s, br, $J_{\text{PW}} = 254$).

Data for Compound 4. Anal. Calcd for $\text{C}_{31}\text{H}_{33}\text{Fe}_2\text{O}_9\text{PW}_2$: C, 35.13; H, 3.14. Found: C, 35.00; H, 3.19. ^1H NMR (C_6D_6): δ 4.79, 4.48 (2s, 2 \times 5H, Cp), 3.00–0.50 (m, 22H, Cy), –20.74 (d, $J_{\text{HP}} = 22$, $J_{\text{HW}} = 53$, 1H, WHFe).

Preparation of $[\text{W}_3\text{Cp}_2(\mu_3\text{-H})(\mu\text{-PCy}_2)(\text{CO})_7]$ (5). A solution of $[\text{W}(\text{CO})_6]$ (0.010 g, 0.028 mmol) and compound 1 (0.020 g, 0.027 mmol) in toluene (4 mL) was irradiated with UV-Vis light at 288 K in a Pyrex Schlenk tube for 8 min, while keeping a gentle N_2 purge, to give an orange solution mainly containing a mixture of compound 5 and $[\text{W}_2\text{Cp}_2(\mu\text{-H})(\mu\text{-PCy}_2)(\text{CO})_4]$. After removal of the solvent, the residue was dissolved in the minimum amount of dichloromethane and chromatographed on alumina (activity IV) at 253 K. Elution with dichloromethane/petroleum ether (1/3) gave an orange fraction which yielded, after removal of solvents, compound 5 as an orange microcrystalline solid (0.012 g, 41%). Anal. Calcd for $\text{C}_{29}\text{H}_{33}\text{O}_7\text{PW}_3$: C, 32.37; H, 3.09. Found: C, 32.05; H, 2.92. ^1H NMR (300.13 MHz): δ 5.37 (s, 10H, Cp), 2.50–1.10 (m, 22H, Cy), –7.78 (s, $J_{\text{HW}} = 84$, 84, 32, 1H, $\mu_3\text{-H}$). $^{13}\text{C}\{^1\text{H}\}$ NMR: δ 231.6 (d, $J_{\text{PW}} = 5$, 2WCO), 196.0 (s, WCO_{eq}), 191.8 (s, WCO_{ax}), 89.1, 87.8 (2s, Cp), 54.3, 51.8 [2d, $J_{\text{CP}} = 24$, $\text{C}^1(\text{Cy})$], 34.0, 32.5 [2d, $J_{\text{CP}} = 2$, $\text{C}^2(\text{Cy})$], 33.7 [d, $J_{\text{CP}} = 4$, $\text{C}^2(\text{Cy})$], 33.6 [s, $\text{C}^2(\text{Cy})$], 28.20, 28.15 [2d, $J_{\text{CP}} = 12$, $\text{C}^3(\text{Cy})$], 28.12 [d, $J_{\text{CP}} = 10$, $\text{C}^3(\text{Cy})$], 28.0 [d, $J_{\text{CP}} = 11$, $\text{C}^3(\text{Cy})$], 26.6 [s, $2\text{C}^1(\text{Cy})$]. $^{13}\text{C}\{^1\text{H}\}$ NMR (213 K): δ 234.5, 234.3 (2s, WCO), 196.1 (s, $J_{\text{WC}} = 124$, WCO_{eq}), 192.1 (s, WCO_{ax}). $^{31}\text{P}\{^1\text{H}\}$ NMR (213 K): δ 123.9 (s, br, $J_{\text{PW}} = 320$). $^{31}\text{P}\{^1\text{H}\}$ NMR (193 K): δ 123.8 (vbr). $^{31}\text{P}\{^1\text{H}\}$ NMR (163 K): δ 127.6 (br, isomer A), 115.9 (br, isomer B). ^1H NMR (213 K): δ 5.39 (s, 10H, Cp), –7.21 (s, $J_{\text{HW}} = 84$, 84, 32, 1H, $\mu_3\text{-H}$). ^1H

NMR (173 K): δ 5.41 (s, 10H, Cp), –6.96 (s, br, 1H, $\mu_3\text{-H}$). ^1H NMR (163 K): δ 5.41 (s, br, 10H, Cp, isomers A and B), –6.65 (s, br, $\mu_2\text{-H}$, isomer B), –7.05 (s, br, $\mu_3\text{-H}$, isomer A); ratio A/B ca. 4.

Preparation of $[\text{RuW}_2\text{Cp}_3(\mu\text{-PCy}_2)(\text{CO})_4]$ (6). A solution of $[\text{Ru}_2\text{Cp}_2(\text{CO})_4]$ (0.013 g, 0.034 mmol) and compound 1 (0.020 g, 0.027 mmol) in toluene (5 mL) was irradiated with UV-Vis light at 263 K in a Pyrex Schlenk tube for 5 min, while keeping a gentle N_2 purge, to give a purple solution. After removal of the solvent, the residue was dissolved in the minimum amount of dichloromethane and chromatographed on alumina (activity IV) at 263 K. Elution with dichloromethane/petroleum ether (2/1) gave an orange fraction which yielded, after removal of solvents, compound 6 as an orange microcrystalline solid (0.020 g, 76%). Anal. Calcd for $\text{C}_{31}\text{H}_{37}\text{O}_4\text{PRuW}_2$: C, 38.25; H, 3.83. Found: C, 38.52; H, 4.11. ^1H NMR (233 K): δ 5.44, 5.04, 5.03 (3s, 3 \times 5H, Cp), 2.60–0.90 (m, 22H, Cy). $^{13}\text{C}\{^1\text{H}\}$ NMR (233 K): 231.2, 224.4, 215.8 (3s, WCO), 205.5 (s, RuCO), 91.9, 90.8, 86.5 (3s, Cp), 59.9 [d, $J_{\text{CP}} = 12$, $\text{C}^1(\text{Cy})$], 55.1 [d, $J_{\text{CP}} = 22$, $\text{C}^1(\text{Cy})$], 38.0, 35.0 [2s, $\text{C}^2(\text{Cy})$], 34.9 [d, $J_{\text{CP}} = 5$, $\text{C}^2(\text{Cy})$], 34.8 [d, $J_{\text{CP}} = 3$, $\text{C}^2(\text{Cy})$], 29.6 [d, $J_{\text{CP}} = 9$, $\text{C}^3(\text{Cy})$], 28.9 [d, $J_{\text{CP}} = 10$, $\text{C}^3(\text{Cy})$], 28.4 [d, $J_{\text{CP}} = 11$, $2\text{C}^3(\text{Cy})$], 27.0, 26.9 [2s, $\text{C}^4(\text{Cy})$].

Preparation of Compound $[\text{Cu}_2\text{W}_2\text{Cp}_2(\mu\text{-H})_3(\mu\text{-PCy}_2)(\text{CO})_2(\text{PPh}_3)_2]$ (7). A solution of $[\text{Cu}(\text{BH}_4)(\text{PPh}_3)_2]$ (0.080 g, 0.133 mmol) and compound 1 (0.030 g, 0.040 mmol) in THF (4 mL) was placed in a Schlenk tube equipped with a Teflon Young's valve, and the mixture was stirred for 24 h to give an orange-brown solution. After removal of the solvent, the residue was dissolved in dichloromethane/petroleum ether (1/1) and chromatographed on alumina (activity IV) at 263 K. Elution with the same solvent mixture gave an orange fraction which yielded, after removal of solvents, compound 7 as an orange microcrystalline solid (0.049 g, 87%). This compound was shown (by NMR) to exist in solution as an equilibrium mixture of two isomers M and N, with the ratio M/N being ca. 10 in C_6D_6 solution and ca. 6 in CD_2Cl_2 solution. Anal. Calcd for $\text{C}_{60}\text{H}_{65}\text{Cu}_2\text{O}_2\text{P}_3\text{W}_2$: C, 51.26; H, 4.66. Found: C, 50.92; H, 4.35. ν_{CO} (petroleum ether): 1772 (m), 1757 (w), 1721 (vs).

Data for Isomer 7M. $^{31}\text{P}\{^1\text{H}\}$ NMR (C_6D_6): δ 45.0 (d, $J_{\text{PP}} = 5$, $J_{\text{PW}} = 240$, 182, $\mu\text{-PCy}_2$), 15.5, 13.3 (2s, br, Cu–P). ^1H NMR (C_6D_6): δ 7.75–7.40 (m, 15H, Ph), 7.05–6.90 (m, 15H, Ph), 5.09, 5.01 (2s, 2 \times 5H, Cp), 2.60–0.80 (m, 22H, Cy), –8.4 (tt, $J_{\text{HH}} = J_{\text{H-PW}} = 8$, $J_{\text{H-PCu}} = J_{\text{H-PCu}} < 1$, $J_{\text{HW}} = 78$, 1H, $\mu\text{-H}$), –9.28 (qt, $J_{\text{HH}} = J_{\text{HH}} = J_{\text{H-PW}} = 8$, $J_{\text{H-PCu}} = J_{\text{H-PCu}} < 1$, $J_{\text{HW}} = 65$, 1H, $\mu\text{-H}$), –9.60 (ddd, $J_{\text{H-PW}} = 20$, $J_{\text{HH}} = 8$, $J_{\text{H-PCu}} = 3$, $J_{\text{HW}} = 51$, 1H, $\mu\text{-H}$).

Data for Isomer 7N. $^{31}\text{P}\{^1\text{H}\}$ NMR (C_6D_6): δ 31.6 (dd, $J_{\text{PP}} = 9$, 5, $J_{\text{PW}} = 203$, $\mu\text{-PCy}_2$), 15.1, 13.3 (2s, br, Cu–P). ^1H NMR (C_6D_6): δ 7.95–7.45 (m, 15H, Ph), 7.10–6.90 (m, 15H, Ph, partially obscured by resonances of major isomer), 4.87 (s, 10H, Cp), –10.47 (dq, $J_{\text{HH}} = 8$, $J_{\text{HPW}} = 4$, 2H, $\mu\text{-H}$), –12.69 (ddt, $J_{\text{H-PW}} = 28$, $J_{\text{H-PCu}} = 18$, $J_{\text{HH}} = J_{\text{HH}} = 8$, 1H, $\mu\text{-H}$); the Cy resonances were obscured by those of the major isomer. The assignments of the different H–P couplings were verified with the aid of selective $^1\text{H}\{^{31}\text{P}\}$ NMR experiments.

X-ray Structure Determination for Compounds 3 and 4. The X-ray intensity data were collected at 100 K on a Kappa-Appex-II Bruker diffractometer, using graphite-monochromated Mo $K\alpha$ radiation. The software APEX³⁶ was used for collecting frames with the omega/phi scans measurement method, and the Bruker SAINT software was used for the data reduction,³⁷ and a multiscan absorption correction was applied with SADABS.³⁸ Using the program suite WinGX,³⁹ the structures were solved by Patterson interpretation and phase expansion using SHELXL97, and refined with full-matrix least-squares on F^2 , using SHELXL97.⁴⁰ For compound 4, a cyclohexyl group was found to be disordered in two positions, and was modeled by introducing 10 C atoms instead of 6 C atoms (sharing two positions) with occupancy factors of 0.6/0.40. Some restraints in the distances and angles were necessary to obtain a convenient model; moreover, one of the cyclopentadienyl carbons [C(12)] had to be refined in combination with the DELU and SIMU instructions. The latter procedure was also applied to the cyclopentadienyl carbon C(18) in compound 3. For both compounds, all the positional parameters and the anisotropic temperature factors of all the non-H

atoms were refined anisotropically, except for the four C atoms involved in the disorder of 4, which were refined isotropically, because some of their temperature factors were persistently nonpositive definites. All H atoms were fixed at calculated positions except for the hydride ligands in both compounds. The atom H(1) in complex 4 was located in the Fourier maps and refined isotropically. In compound 3, the hydride ligand was found to be disordered in two positions. The first one, labeled H(1), could be located in the Fourier map and refined isotropically. The other part of the disordered hydride could not be located in the final difference map, therefore possible positions were investigated by a potential energy minima search using the program XHYDEX.⁴¹ Only one minimum was found in the Fe(1)–Fe(2)–W(2) face, so that one was assigned to the second position of the disordered hydride and labeled H(2). Nevertheless, it had to be fixed in order to reach a satisfactory refinement. An occupation factor of 50% was given to each of the hydride positions. Further crystallographic data and structure refinement details are collected in Table 4.

■ ASSOCIATED CONTENT

■ Supporting Information

CIF file containing full crystallographic data for compounds 3 and 4. This material is available free of charge via the Internet at <http://pubs.acs.org>.

■ AUTHOR INFORMATION

Corresponding Author

*E-mail: mara@uniovi.es.

Notes

The authors declare no competing financial interest.

■ ACKNOWLEDGMENTS

We thank the DGI of Spain for financial support (Project Nos. CTQ2009-09444 and CTQ2012-33187) and a grant to M.F.V., and we thank the Consejería de Educación del Principado de Asturias for a grant to A.T.

■ REFERENCES

- (1) (a) Johnson, B. F. G.; Lewis, J.; Kilty, P. A. *J. Chem. Soc. A* **1968**, 2859–2864. (b) Burgess, K. *Polyhedron* **1984**, *3*, 1175–1225. (c) Deeming, A. J. *Adv. Organomet. Chem.* **1986**, *26*, 1–96. (d) Smith, A. K. In *Comprehensive Organometallic Chemistry*, 2nd Edition; Abel, E. W., Stone, F. G. A., Wilkinson, G., Eds.; Pergamon: Oxford, U.K., 1995; Vol. 7, Chapter 13. (e) Raithby, P. R.; Johnson, A. L. In *Comprehensive Organometallic Chemistry*, 3rd Edition; Mingos, D. M. P., Crabtree, R. H., Eds.; Elsevier: Oxford, U.K., 2007; Vol. 6 (Bruce, M., Ed.), Chapters 18 and 19.
- (2) (a) Bennett, M. J.; Graham, W. A. G.; Hoyano, J. K.; Hutcheon, W. L. *J. Am. Chem. Soc.* **1972**, *94*, 6232–6233. (b) D'Alfonso, G. *Chem.—Eur. J.* **2000**, *6*, 209–215.
- (3) (a) Riera, V.; Ruiz, M. A.; Tiripicchio, A.; Tiripicchio-Camellini, M. *J. Chem. Soc., Chem Commun.* **1985**, 1505–1507. (b) García-Alonso, F. J.; García-Sanz, M.; Riera, V.; Ruiz, M. A.; Tiripicchio, A.; Tiripicchio-Camellini, M. *Angew. Chem., Int. Ed. Engl.* **1988**, *27*, 1167–1168. (c) Liu, X. L.; Riera, V.; Ruiz, M. A.; Lanfranchi, M.; Tiripicchio, A. *Organometallics* **2003**, *22*, 4500–4510 and references therein. (d) García, M. E.; Melón, S.; Ruiz, M. A.; Marchiò, L.; Tiripicchio, A. *J. Organomet. Chem.* **2011**, *696*, 559–567. (e) Alvarez, M. P.; Alvarez, M. A.; Carreño, R.; Ruiz, M. A.; Bois, C. *J. Organomet. Chem.* **2011**, *696*, 1736–1748.
- (4) Suzuki, H. *Eur. J. Inorg. Chem.* **2002**, 1009, 1023 and references therein.
- (5) Süß-Fink, G.; Therrien, B. *Organometallics* **2007**, *26*, 766–774 and references therein.
- (6) (a) Alvarez, C. M.; Alvarez, M. A.; García, M. E.; Ramos, A.; Ruiz, M. A.; Lanfranchi, M.; Tiripicchio, A. *Organometallics* **2005**, *24*, 7–9. (b) Alvarez, M. A.; García, M. E.; Ramos, A.; Ruiz, M. A.

Organometallics **2006**, *25*, 5374–5380. (c) Alvarez, C. M.; Alvarez, M. A.; García, M. E.; Ramos, A.; Ruiz, M. A.; Graiff, C.; Tiripicchio, A. *Organometallics* **2007**, *26*, 321–331. (d) Alvarez, M. A.; García, M. E.; Ramos, A.; Ruiz, M. A. *Organometallics* **2007**, *26*, 1461–1472. (e) Alvarez, M. A.; García, M. E.; Ramos, A.; Ruiz, M. A.; Lanfranchi, M.; Tiripicchio, A. *Organometallics* **2007**, *26*, 5454–5467. (f) García, M. E.; Ramos, A.; Ruiz, M. A.; Lanfranchi, M.; Marchiò, L. *Organometallics* **2007**, *26*, 6197–6212.

(7) (a) Hoffmann, R. *Angew. Chem., Int. Ed. Engl.* **1982**, *21*, 711–724. (b) Stone, F. G. A. *Angew. Chem., Int. Ed. Engl.* **1984**, *23*, 89–99.

(8) (a) Srinivasan, P.; Leong, W. K. *J. Organomet. Chem.* **2006**, *691*, 403–412. (b) Pereira, L.; Leong, W. K.; Wong, S. Y. *J. Organomet. Chem.* **2000**, *609*, 104–109. (c) Hung, S. Y. W.; Wong, W. T. *J. Organomet. Chem.* **1998**, *566*, 237–243. (d) Au, Y. K.; Wong, W. T. *J. Chem. Soc., Dalton Trans.* **1996**, 899–911. (e) Hsu, L. Y.; Hsu, W. L.; McCarthy, D. A.; Krause, J. A.; Chung, J. H.; Shore, S. G. *J. Organomet. Chem.* **1992**, *426*, 121–130. (f) Park, J. T.; Cho, J. J.; Chun, K. M.; Yun, S. S. *J. Organomet. Chem.* **1992**, *433*, 295–303. (g) Colombie, A.; McCarthy, D. A.; Krause, J.; Hsu, L. Y.; Hsu, W. L.; Jan, D. Y.; Shore, S. G. *J. Organomet. Chem.* **1990**, *383*, 421–440. (h) Jan, D. Y.; Coffy, T. J.; Hsu, W. L.; Shore, S. G. *Inorg. Synth.* **1989**, *25*, 195–199. (i) Martin, L. R.; Einstein, F. W. B.; Pomeroy, R. K. *Organometallics* **1988**, *7*, 294–304. (j) Jan, D. Y.; Hsu, L. Y.; Hsu, W. L.; Shore, S. G. *Organometallics* **1987**, *6*, 274–283. (k) Noren, B.; Sundberg, P. *J. Chem. Soc., Dalton Trans.* **1987**, 3103–3105. (l) Chi, Y.; Shapley, J. R.; Churchill, M. R.; Li, Y. *J. Inorg. Chem.* **1986**, *25*, 4165–4170. (m) Bruce, M. L.; Horn, E.; Matison, J. G.; Snow, M. R. *J. Organomet. Chem.* **1985**, *286*, 271–287. (n) Farrugia, L. J.; Howard, J. A. K.; Mitrprachachon, P.; Stone, F. G. A.; Woodward, P. *J. Chem. Soc., Dalton Trans.* **1981**, 155–161. (o) Plotkin, J. S.; Alway, D. G.; Weisenberger, C. R.; Shore, S. G. *J. Am. Chem. Soc.* **1980**, *102*, 6156–6157. (p) Farrugia, L. J.; Howard, J. A. K.; Mitrprachachon, P.; Spencer, J. L.; Stone, F. G. A.; Woodward, P. *J. Chem. Soc., Chem. Commun.* **1978**, 260–262.

(9) (a) Huang, S. H.; Watson, W. H.; Carrano, C. J.; Wang, X.; Richmond, M. G. *Organometallics* **2010**, *29*, 61–75. (b) Comstock, M. C.; Prussak-Wieckowska, T.; Wilson, S. R.; Shapley, J. R. *Inorg. Chem.* **1997**, *36*, 4397–4404. (c) Bergamo, M.; Beringhelli, T.; D'Alfonso, G.; Mercandelli, P.; Moret, M.; Sironi, A. *Organometallics* **1997**, *16*, 4129–4137. (d) Bergamo, M.; Beringhelli, T.; D'Alfonso, G.; Ciani, G.; Moret, M.; Sironi, A. *Organometallics* **1996**, *15*, 3876–3884. (e) Beringhelli, T.; Ciani, G.; D'Alfonso, G.; Garlaschelli, L.; Moret, M.; Sironi, A. *J. Chem. Soc., Dalton Trans.* **1992**, 1865–1866. (f) Antognazza, P.; Beringhelli, T.; D'Alfonso, G.; Minoja, A.; Ciani, G.; Moret, M.; Sironi, A. *Organometallics* **1992**, *11*, 1777–1784. (g) Ciani, G.; Moret, M.; Sironi, A.; Antognazza, P.; Beringhelli, T.; D'Alfonso, G.; Della Pergola, R.; Minoja, A. *J. Chem. Soc., Chem. Commun.* **1991**, 1255–1257. (h) Beringhelli, T.; Ceriotti, A.; D'Alfonso, G.; Della Pergola, R.; Ciani, G.; Moret, M.; Sironi, A. *Organometallics* **1990**, *9*, 1053–1059.

(10) (a) Carreño, R.; Riera, V.; Ruiz, M. A.; Bois, C.; Jeannin, Y. *Organometallics* **1992**, *11*, 4022–4028. (b) Carreño, R.; Riera, V.; Ruiz, M. A.; Bois, C.; Jeannin, Y. *Organometallics* **1992**, *11*, 2923–2930. (c) Riera, V.; Ruiz, M. A.; Tiripicchio, A.; Tiripicchio-Camellini, M. *Organometallics* **1993**, *12*, 2962–2972. (d) Carreño, R.; Riera, V.; Ruiz, M. A.; Lanfranchi, M.; Tiripicchio, A.; Tiripicchio-Camellini, M. *Organometallics* **1994**, *13*, 993–1004.

(11) Alvarez, M. A.; García, M. E.; García-Vivó, D.; Ruiz, M. A.; Vega, M. F. *Organometallics* **2010**, *29*, 512–515.

(12) See, for example: (a) Shriver, D. F.; Kaesz, H. D.; Adams, R. D. *The Chemistry of Metal Cluster Complexes*; VCH: Weinheim, Germany, 1990. (b) Adams, R. D.; Cotton, F. A. *Catalysis by Di- and Polynuclear Metal Complexes*; Wiley–VCH: New York, 1998. (c) Braunstein, P.; Oro, L. A.; Raithby, P. R. *Metal Clusters in Chemistry*; Wiley–VCH: Weinheim, Germany, 1999; Vols. 1 and 2.

(13) Rothenberg, G. *Catalysis: Concepts and Green Applications*; Wiley–VCH: Weinheim, Germany, 2008.

(14) García, M. E.; Riera, V.; Rueda, M. T.; Ruiz, M. A.; Sáez, D. *Organometallics* **2002**, *21*, 5515–5525.

- (15) Lindner, E.; Stängle, M.; Hiller, W.; Fawzi, R. *Chem. Ber.* **1988**, *121*, 1421–1426.
- (16) Mays, M. J.; Raithby, P. R.; Sarveswaran, K.; Solan, G. A. *J. Chem. Soc., Dalton Trans.* **2002**, 1671–1677.
- (17) Alvarez, M. A.; García, M. E.; Riera, V.; Ruiz, M. A. *Organometallics* **1999**, *18*, 634–641.
- (18) Alvarez, M. A.; García, M. E.; Martínez, M. E.; Ruiz, M. A. *Organometallics* **2010**, *29*, 904–916.
- (19) García, M. E.; García-Vivó, D.; Ruiz, M. A. *Organometallics* **2009**, *28*, 4385–4393.
- (20) W_2Fe_2 clusters: (a) Mansour, M. A.; Curtis, M. D.; Kampf, J. W. *Organometallics* **1997**, *16*, 275–284. (b) Konchenko, S. N.; Virovets, A. V.; Podberezskaya, N. V. *Polyhedron* **1997**, *16*, 1689–1691.
- (21) W_2Ru_2 clusters: (a) Chi, Y.; Liu, L. K.; Huttner, G.; Zsolnai, L. *J. Organomet. Chem.* **1990**, *390*, C50–C56. (b) Hwang, D. K.; Lin, P. J.; Chi, Y.; Peng, S. M.; Lee, G. H. *J. Chem. Soc., Dalton Trans.* **1991**, 2161–2167.
- (22) W_2Os_2 cluster: Chi, Y.; Wu, C. H.; Peng, S. M.; Lee, G. H. *Organometallics* **1991**, *10*, 1676–1682.
- (23) Braterman, P. S. *Metal Carbonyl Spectra*; Academic Press: London, U.K., 1975.
- (24) According to the modified Eyring equation $\Delta G^\ddagger_{T_c} = 19.14T_c[9.97 + \log(T_c/\Delta\nu)]$ (J/mol). See: Günter, H. *NMR Spectroscopy*; John Wiley: Chichester, U.K., 1980; p 243.
- (25) Mathur, P.; Ghose, S.; Hossain, M. M.; Satyanarayana, C. V. V.; Drake, J. E. *J. Organomet. Chem.* **1998**, *557*, 221–225.
- (26) (a) Jeffery, J. C.; Lawrence-Schmidt, J. G. *J. Chem. Soc., Chem. Commun.* **1986**, 17–19. (b) Jeffery, J. C.; Lawrence-Schmidt, J. G. *J. Chem. Soc., Dalton Trans.* **1990**, 1589–1596.
- (27) Carty, A. J.; MacLaughlin, S. A.; Nucciarone, D. In *Phosphorus-31 NMR Spectroscopy in Stereochemical Analysis*; Verkade, J. G., Quin, L. D., Eds.; VCH: Deerfield Beach, FL, 1987; Chapter 16.
- (28) Jameson, C. J. in *Phosphorus-31 NMR Spectroscopy in Stereochemical Analysis*; Verkade, J. G.; Quin, L. D., Eds.; VCH: Deerfield Beach, FL, 1987, Chapter 6.
- (29) Geoffroy, G. L.; Wrighton, M. S. *Organometallic Photochemistry*; Academic Press: New York, 1979.
- (30) Alvarez, M. A.; García, M. E.; Ramos, A.; Ruiz, M. A. *J. Organomet. Chem.* **2009**, *695*, 36–44.
- (31) Salter, I. D. *Adv. Organomet. Chem.* **1989**, *29*, 249–343. (b) Salter, I. D. In *Comprehensive Organometallic Chemistry*, 2nd Edition; Abel, E. W., Stone, F. G. A., Wilkinson, G., Eds.; Pergamon: Oxford, U.K., 1995; Vol. 10, Chapter 5.
- (32) Armarego, W. L. F.; Chai, C. *Purification of Laboratory Chemicals*, 5th Edition; Butterworth–Heinemann: Oxford, U.K., 2003.
- (33) Herrmann, W. A. *Angew. Chem.* **1974**, *86*, 345–356.
- (34) Humphries, A. P.; Knox, S. A. R. *J. Chem. Soc., Dalton Trans.* **1975**, 1710–1714.
- (35) Cariati, F.; Naldini, L. *Gazz. Chim. Ital.* **1965**, *95*, 3–15.
- (36) APEX 2, Version 2.0-1; Bruker AXS, Inc.: Madison, WI, 2005.
- (37) SMART & SAINT Software Reference Manuals, Version 5.051 (Windows NT Version); Bruker Analytical X-ray Instruments: Madison, WI, 1998.
- (38) Sheldrick, G. M. *SADABS, Program for Empirical Absorption Correction*; University of Göttingen: Göttingen, Germany, 1996.
- (39) Farrugia, L. J. *J. Appl. Crystallogr.* **1999**, *32*, 837–838.
- (40) Sheldrick, G. M. *Acta Crystallogr., Sect. A: Found Crystallogr.* **2008**, *64*, 112–122.
- (41) Orpen, A. G. *J. Chem. Soc., Dalton Trans.* **1980**, 2509–2516.